Nanoscale

Cite this: *Nanoscale*, 2012, **4**, 4247

www.rsc.org/nanoscale

**PAPER**

# Bright two-photon emission and ultra-fast relaxation dynamics in a DNA-templated nanocluster investigated by ultra-fast spectroscopy

**Sung Hei Yau,[a] Neranga Abeyasinghe,[a] Meghan Orr,[a] Leslie Upton,[a] Oleg Varnavski,[a] James H. Werner,[b] Hsin-Chih Yeh,[b] Jaswinder Sharma,[b] Andrew P. Shreve,[c] Jennifer S. Martinez[b] and Theodore Goodson III*[a]**

***Received 15th March 2012, Accepted 1st May 2012***
**DOI: 10.1039/c2nr30628j**



Metal nanoclusters have interesting steady state fluorescence emission, two-photon excited emission and ultrafast dynamics. A new subclass of fluorescent silver nanoclusters (Ag NCs) are NanoCluster Beacons. NanoCluster Beacons consist of a weakly emissive Ag NC templated on a single stranded DNA ("Ag NC on ssDNA") that becomes highly fluorescent when a DNA enhancer sequence is brought in proximity to the Ag NC by DNA base pairing ("Ag NC on dsDNA"). Steady state fluorescence was observed at 540 nm for both Ag NC on ssDNA and dsDNA; emission at 650 nm is observed for Ag NC on dsDNA. The emission at 550 nm is eight times weaker than that at 650 nm. Fluorescence up-conversion was used to study the dynamics of the emission. Bi-exponential fluorescence decay was recorded at 550 nm with lifetimes of 1 ps and 17 ps. The emission at 650 nm was not observed at the time scale investigated but has been reported to have a lifetime of 3.48 ns. Two-photon excited fluorescence was detected for Ag NC on dsDNA at 630 nm when excited at 800 nm. The two-photon absorption cross-section was calculated to be ~3000 GM. Femtosecond transient absorption experiments were performed to investigate the excited state dynamics of DNA–Ag NC. An excited state unique to Ag NC on dsDNA was identified at ~580 nm as an excited state bleach that related directly to the emission at 650 nm based on the excitation spectrum. Based on the optical results, a simple four level system is used to describe the emission mechanism for Ag NC on dsDNA.

## I. Introduction

Metal nanoparticles are comprised of a small number of metal atoms and can be classified as either nanoparticles or nanoclusters based upon their size.[1–4] Metal nanoparticles have a metal core of ~3 nm to tens of nm, whereas systems smaller than ~3 nm are considered nanoclusters.[1–8] Recently, a relatively intensified research effort has been devoted to the synthesis and characterization of nanoclusters, due to their potential applications in catalysis,[9–15] as medical imaging markers,[16,17] and their use in molecular electronics.[9,18] While a number of nanocluster systems have been investigated, gold mono-layered protected metal clusters (MPCs) are perhaps the most studied and best understood systems. In particular, the structures of a number of gold MPCs have been determined by X-ray crystallography and the syntheses of these nanoclusters are well-established.[1–4,19–27] Studies of gold MPCs lay an important foundation for understanding the inherent properties of other metal nanocluster systems.

In our previous work with gold MPCs $Au_{25}$, we discovered a number of interesting effects, which are not present in larger gold nanoparticles. In particular, we found that the gold MPCs possessed strong two-photon excited emission, which could lead to applications in imaging and detection areas.[7,8,16,17] We also found that as the size of the clusters was reduced from ~5 nm to ~2 nm, the fluorescence lifetime and the excited state lifetimes increased, clear indicators of quantum confinement effects. This change in the lifetime showed a sharp shift when we reached a size of ~2 nm and suggested a change in the mechanism of excitation and emission in the small gold clusters. This was explained by a simple model which relates to a band edge opening and the creation of "molecular-like" states at smaller cluster sizes which was also evident in the steady-state UV-Vis absorption spectra.[4,8,28–32] An interesting question stems from these results with gold: is this observed shift in mechanism of emission and excitation common for other metal nanoclusters? In order to seek answers to this question we turn our attention to silver. Silver and gold are both noble and free electron metals that contribute one free electron per atom. Synthetic routes for silver MPCs have been reported in the literature and are similar to gold MPC synthesis.[33,34] Additionally, based on results

[a]*Department of Chemistry, University of Michigan, Ann Arbor, Michigan, 48109, USA. E-mail: tgoodson@umich.edu*
[b]*Center for Integrated Nanotechnologies, Los Alamos National Laboratory, Los Alamos, New Mexico 87545, USA*
[c]*Department of Chemical and Nuclear Engineering, University of New Mexico, Albuquerque, NM 87196, USA*

suggested by invoking the "super atom theory"[4] for MPCs, silver systems should follow similar geometries and the rules of "magic numbers".[4,33] It is also reasonable for one to hypothesize that silver nanoclusters will behave like gold nanoclusters. There has been much advancement in the synthesis of silver MPCs,[33,34] including recent work done by the Bigioni group,[33] to produce a family of discrete-sized silver nanoclusters.

Previous studies on gold nanoclusters have excited enthusiasm for investigations of other metal cluster systems in an attempt to further understand the general picture of emission and excitations in small metal clusters. In this contribution we investigate metal nanoclusters that are stabilized by DNA.[35–46] One of the most exciting aspects of these systems is that DNA-based systems give rise to many possible applications in the field of bio-imaging and ultra-sensitive detection of biological agents.[38] DNA-Templated Fluorescence Silver Nanoclusters (DNA–Ag NCs)[35–44] are silver nanoclusters nested in single stranded DNA and can be considered as NanoCluster Beacons.[36] DNA–Ag NCs are highly stable systems with tunable fluorescence dependent on the DNA scaffold composition.[35–38] A new subclass of DNA–Ag NCs are NanoCluster Beacons which consist of a poorly emissive Ag NC on a single DNA strand (so-called "Ag NCs on ssDNA" in this text), whose fluorescence is greatly enhanced when brought in proximity to a tunable enhancer sequence (the resulting system is called "Ag NCs on dsDNA" in this manuscript as the enhancer is held in proximity to the Ag NC by base pairing).[36] The NanoCluster Beacons ("Ag NC on dsDNA") have a quantum yield of approximately 30% per activated cluster, as determined by the gradient method in a fluorimeter with cresyl violet as the standard.[47]

Traditionally, metal MPC systems have been characterized by mass spectrometry and shell substitutions to fully account for the core metal and outer shell ligand number; for DNA Ag NC systems, elemental analysis and mass spectrometry have been utilized to estimate the number of atoms.[44–46] Unfortunately, these methods report the average number of silver atoms within a DNA strand and not necessarily the number of atoms within a nanocluster. Instead, Ag K-edge Extended X-ray Absorption Fine Structure (EXAFS) has been used to identify the DNA–Ag nanocluster size and to demonstrate metal–metal and metal–ligand bonding.[36] From this analysis, Ag NCs have been shown to contain Ag–DNA bonds and Ag–Ag bonds at distances consistent with nanoclusters. Also, the EXAFS analysis estimated the cluster size to be between 8 and 20 atoms, depending on the DNA template,[37] although the exact cluster size and geometry are at present unknown.

In a previous publication, we focused on the emission mechanism of Au MPCs, and used a three-level system[19,28,48,49] to model the two different emissions of Au MPCs.[8] Specifically we associated the short-lived emission to be related to the core, and the longer-lived emission to come from a "surface state" of MPCs. In a similar manner, we investigate the steady state absorption and emission from nanoclusters templated on ssDNA and the same nanoclusters duplexed into dsDNA. Time-resolved emission was investigated with the aid of ultrafast fluorescence up-conversion. Given the large two-photon response for $Au_{25}$, we also studied the emission of DNA–Ag NCs from two-photon absorption at 800 nm. Transient absorption was used to probe the excited state dynamics of the system. In this work, we aim to understand the emission mechanism of DNA–Ag NCs.

## II. Experimental

### A. Sample preparation

All DNA strands were purchased from Integrated DNA Technologies Incorporated and were purified by desalting. ssDNA (Ag NC bearing strand: 5′-CCC TTAAT CCCC TAT AAT AAA TTT TAA ATA TTA TTT ATT AAT) was first dissolved in ultrapure deionized water. Ag NCs were formed by addition of $AgNO_3$ (99.9%, Sigma-Aldrich) to the DNA solution, followed by reduction with $NaBH_4$. Final concentrations were 100 μM DNA, 1.2 mM $AgNO_3$, and 1.2 mM $NaBH_4$ in 20 mM sodium phosphate buffer (pH 6.6). The aqueous solution of $NaBH_4$ was prepared by dissolving $NaBH_4$ powder in water and adding the required volume to the DNA–$Ag^+$ mixture within 30 seconds, followed by vigorous shaking for 5 seconds. The reaction was kept in the dark at room temperature for 18 hours, filtered, and frozen for transport. dsDNA–Ag NCs were produced at room temperature by mixing ssDNA–Ag NC with an excess of the complementary strand containing a guanine rich enhancer sequence (5′-ATT AAT AAA TAA TAT TTA AAA TTT ATT ATA GGGTGGGGTGGGGTGGGG). Absorption spectra were taken 40 min after hybridization. The resultant dsDNA samples were used without further purification or alteration.

### B. Steady state absorption and emission

Steady state absorption and emission measurements were performed at room temperature, with a 1 mm thick quartz sample cell. Optical absorption measurements were carried out using an Agilent 8432 UV-Vis absorption spectrometer. Fluorescence measurements were carried out using a Fluoromax-2 spectrofluorophotometer. UV-Vis spectra were compared before and after the experiment to ensure no appreciable photo-degradation occurred during the measurements.

### C. Femtosecond transient absorption measurements

Transient absorption was used to investigate the excited state dynamics of metal nanoclusters, the experimental setup of which has been described previously.[50] The experiments were carried out in the visible region using an ultrafast pump-probe spectrometer. A Millennia pumped Ti:sapphire oscillator (Spectra Physics, Tsunami) was used to generate 100 fs, 1 mJ pulses at 800 nm with an Ti:sapphire regenerative amplifier (Spectra Physics, Spitfire). The output beam was split with a beam splitter, creating pump and probe beam pulses (85% and 15%). The pump beam was produced using an optical parametric amplifier (OPA-800), with a pump range of 300 nm to 1200 nm. For this work, the pump beam was set at 470 nm, generated by the fourth harmonic of the idler. The white light probe beam was generated from the amplifier output guided into a Helios system made by Ultrafast Systems Inc. The probe beam was generated by a 2 mm sapphire plate from 450 nm to 750 nm, and time delayed with a computer-controlled motion controller. The white light was then overlapped with the pump beam in a 2 mm quartz cuvette containing the sample and the change in absorbance for the signal was collected by a CCD detector (Ocean Optics). Data acquisition was controlled by software from Ultrafast Systems Inc. The typical power of the probe beam was <0.1 μJ, while the

 

pump beam used was around ~0.1 to 0.4 μJ per pulse. The sample was stirred with a rotating magnetic stirrer and no photo-degradation of the sample was observed.

### D. Femtosecond time-resolved fluorescence

The time-resolved fluorescence experiments were carried out using a fluorescence up-conversion set-up that has been previously described.[51] The sample solution was excited with frequency-doubled light from a mode-locked Ti:sapphire femtosecond laser (Tsunami, Spectra Physics) pumped by a Nd–YLF laser (Millenia X, Spectra Physics). This produces pulses of ~100 fs duration in a wavelength range of 385–430 nm. The polarization of the excitation beam for the anisotropy measurements was controlled with a Berek compensator. The horizontally polarized fluorescence emitted from the sample was up-converted in a nonlinear crystal of β-barium borate using a pump beam at ~800 nm that was first passed through a variable delay line. This system acts as an optical gate and enables the fluorescence to be resolved temporally. Spectral resolution was achieved by dispersing the up-converted light in a monochromator and detecting it using a photomultiplier tube (R1527P, Hamamatsu, Hamamatsu City, Japan). The instrument response function (IRF) has a duration of ~200 fs for visible excitation. The energy per excitation pulse did not exceed 600 pJ for any experiment. Standard dyes were used to calibrate the system. Lifetimes of the fluorescence decay were obtained by fitting the experimental profile with multi-exponential decay functions convoluted with the IRF.

### E. Two-photon excited fluorescence

Two-photon absorption cross-sections were measured using the two-photon excited fluorescence (TPEF) method as described elsewhere.[52] A Kapteyn Murnane Laboratories diode-pumped mode-locked Ti:sapphire laser was utilized for sample excitation. The bandwidth at 800 nm was 47 nm, and the pulse duration was 30 fs. The input power from the laser was varied by using a variable neutral density filter and focused onto the sample cell (quartz cuvette, 0.4 cm path length). The focusing lens has a focal length of 11.5 cm. The resultant fluorescence was collected perpendicular to the incident beam. An iris was placed prior to the neutral density filter in order to ensure a circular beam. A 1 in. focal length plano-convex lens was used to direct the collected fluorescence into a monochromator whose output was coupled to a photomultiplier tube. The photons were converted into counts by a photon-counting unit. A logarithmic plot of collected fluorescence photons *versus* input power was verified to yield a slope of 2 indicating the quadratic power dependence. A comparison of the fluorescence intensity of the nanoclusters relative to a dye of known two-photon cross-section was used to measure the two photon cross-section of the nanoclusters.

## III. Results and discussion

### A. Steady state absorption

The steady state absorption spectra are shown in Fig. 1 for various Ag nanoparticles (NPs). The absorption spectra for Ag NP (2.2 nm) are Gaussian peaks modeled after published results (using wavelength and spectra width) to demonstrate the surface plasmon response for silver nanoparticles.[52] Surface Plasmon Resonance (SPR) is the coherent oscillation of conduction electrons near NP surfaces and can be seen as a strong and broad optical absorption near the resonance wavelength. It has been reported that as the nanoparticle size decreases, a red shift is observed.[52] Comparison of the SPR absorption peaks and the absorption spectra for Ag NC on ssDNA reveals a similar absorption peak at ~455 nm, suggesting that the solution of Ag NC on ssDNA may contain larger NPs. Pure ssDNA and dsDNA without Ag NC only absorb in the UV range (200 nm–300 nm), and do not affect the (visible) absorption of the DNA–Ag systems. Ag NC on dsDNA was formed directly by the hybridization of Ag NC on ssDNA with an excess of complementary DNA strand with a guanine-rich tail ($3'$-$G_4(TG_4)_2TG_3$). The absorption peaks for Ag NC on ssDNA are different from the peaks for dsDNA at the same concentration. The weak absorption shoulder at ~455 nm is decreased for Ag NC on dsDNA, possibly resulting from dissolution of solution based NPs after addition of excess complementary DNA strand. The red peak shift for the ~400 nm peak also suggests a decreased system size. Two new absorption peaks emerge at 580 nm and 670 nm for Ag NCs on dsDNA; the appearance of discrete absorption features is strong evidence for quantum size effects. The quantum size effect is used to describe the change in electronic states as the size of the metal core decreases. From our previous work,[6–8] we found that as metal nanoparticle size decreases, the metal behaves more like a single molecule or a "super atom". Previous fluorescence reversibility and fluorescence correlation spectroscopy,[36] EXAFS,[37] and the absorption peaks observed in this work are all indicative of Ag NC–DNA nanoclusters.

The absorption spectrum for a hypothetical Ag MPC ($Ag_{25}(SH)_{18}^-$) using $Au_{25}$ geometry and bonding motif has been published.[53] The calculated spectrum shares some similarity to the absorption spectrum of Ag NC on dsDNA, suggesting that the DNA system may be electronically similar to MPCs.

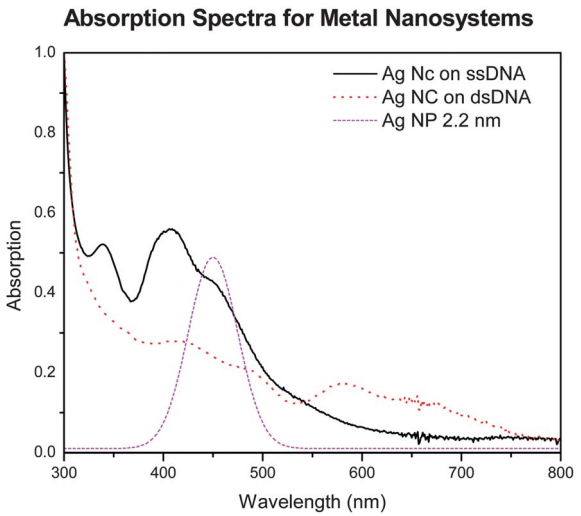


**Fig. 1** Absorption spectrum for metal nanoclusters.

### B. Steady state emission

The normalized steady-state emission for Ag NC on dsDNA (Fig. 2) was studied with excitation at 400 nm and 580 nm. At 400 nm excitation, the emission spectra for Ag NC on ssDNA showed one peak at 550 nm. The emission spectra for Ag NCs on dsDNA excited at 400 nm show two peaks at 540 nm (weak) and 650 nm (strong), additional excitation at 580 nm shows the same peak at 650 nm. The peak at 470 nm under 580 nm excitation is the Raman signal from the solvent. The emission at 650 nm was reported to have a bulk enhancement ratio of 500, and from our steady state measurement, it is eight times stronger than the emission at 550 nm. Typically, the emission from bulk metal is only observable under laser excitation with a lower quantum yield of $10^{-10}$ (Bulk Au).[54] Emission from other DNA based NC systems has been reported to be as high as 0.64.[38] Quantum efficiency of the activated Ag NC on dsDNA at 650 nm was measured to be 0.30,[47] and the quantum efficiency at 550 nm is estimated to be 0.03. The excitation spectrum for the emission at 650 nm is shown in Fig. 3. The strong peak in the excitation spectrum is at 590 nm which corresponds to the 580 nm peak in the absorption spectra that emerges upon hybridization.

### C. Fluorescence up-conversion

Using time-resolved fluorescence up-conversion, we can study the emission dynamics for DNA–Ag NCs. Based on the result from steady state emission (Fig. 2), different emission wavelengths were investigated (Fig. 4a and b) at 550 nm, 600 nm and 650 nm. Time-resolved emission was detected only for 550 nm and 600 nm (Fig. 4a), but not for 650 nm. It is reported that time-correlated single photon counting measurements placed the lifetime for the emission at 650 nm at 3.48 ns.[36] The emission at 650 nm was not detected at the time scale measured (up to 4 ps, with 60 fs resolution), suggesting that the emission at 650 nm comes from a later transition, which will be the focus of future studies. The emission measured at 550 nm and 600 nm exhibits very similar dynamics, with a rise time of 3.85 ps for 550 nm and 2.49 ps for 600 nm (Fig. 4a). The fluorescence decay shows a two-component decay with lifetimes of 1 ps and 17 ps. The longer

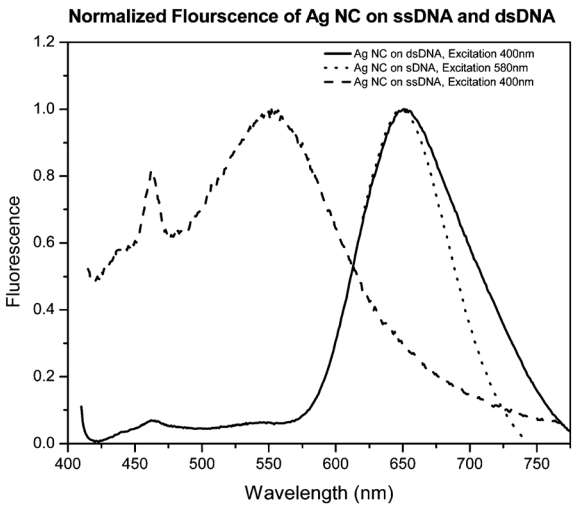


**Fig. 2** Normalized fluorescence spectra for Ag NC on ssDNA and dsDNA under 400 nm and 580 nm excitation.

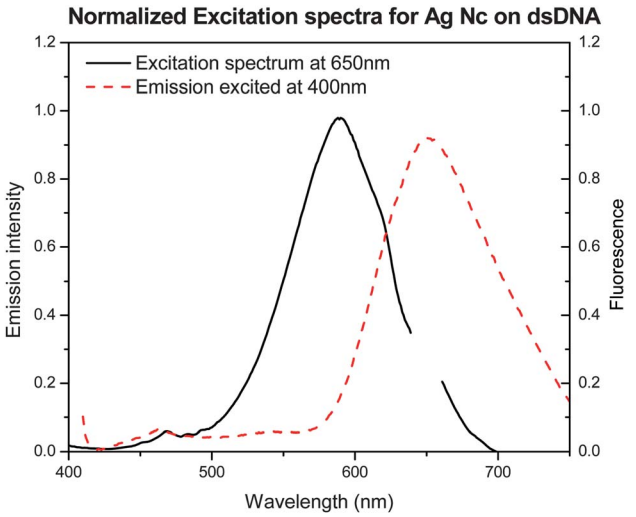


**Fig. 3** Excitation spectra for dsDNA measuring the emission at 650 nm, and the emission spectrum excited at 400 nm.

lifetime at 600 nm is potentially contaminated by the long-lived 650 nm emission, with half the amplitude of 550 nm. The similar rise time for the emission at 550 nm and 600 nm leads us to conclude that the fluorescence from these states originates from the same initial excited state centered. The weak emission feature is common for both Ag NC on dsDNA and ssDNA. Given that the only difference between the two systems is the complementary DNA strand, the emission could be from the common metal core. The observed two-exponential decay (Fig. 4b) is similar to the three-exponential decay reported for larger dendrimer nanocomposites and very different from the single exponential decay expected of nanoclusters.[8,56] However, the lifetimes of 1 ps and 17 ps are much longer than the 70 fs, 700 fs and 5.3 ps lifetimes reported for silver dendrimer nanocomposites.[56] The short lifetime for nanoparticles (and nanocomposites) is reported to be typical for sp–d band hole recombination[55] and the longer lifetime for the DNA–Ag NCs suggests that such recombination is not present. Additionally, the excitation is far from the SPR band, making the emission to be related to the SPR band even less likely. The lifetime analysis suggests that nanoclusters are present but it is possible that other larger nanoparticles can contribute to the bi-exponential decay. Based on the common components of dsDNA and ssDNA and the long lifetime of emission at 550 nm, the emission is from the metal nanoclusters.

The emission from 650 nm could be the result of a triplet state, a charge transfer state or surface states. Based on the published work that detail the emission from Au MPCs,[28,8] the emission from 650 nm is potentially from a surface state, and it is possible that the energy transfer to this state occurs much later than the time scale investigated. Surface state emissions for Au MPCs are reported to be in the NIR region with a quantum yield in the order of $10^{-4}$,[7,8,57–61] three orders of magnitude weaker than the quantum yield of DNA–Ag NCs.

### D. Two-photon absorption

We examined the two-photon absorption (TPA) efficiencies of the DNA–Ag NC at 800 nm excitation (Fig. 5). The log of pump

 

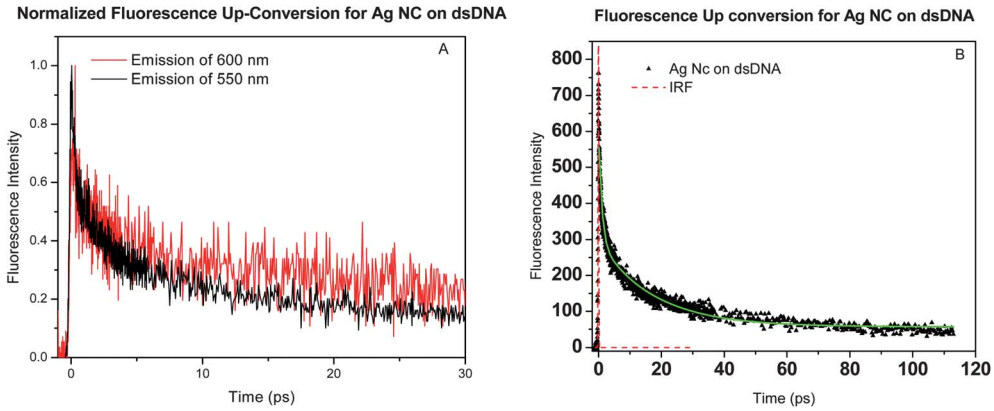


**Fig. 4** (A) Normalized fluorescence up-conversion lifetime for Ag NC on dsDNA at 550 nm and 600 nm. (B) Fluorescence up conversion for Ag NC on dsDNA at 550 nm, fitted with a bi-exponential decay.

power dependence against the log of the fluorescence at 630 nm for the Ag NC on dsDNA is shown in Fig. 6. These data are fitted well by a line of slope two, indicating a two-photon excitation. The method for calculating the TPA cross-section is the comparative two-photon excited fluorescence method with standard reference H2TPP in toluene. The TPA action cross-section at 800 nm for the Ag NC on dsDNA was determined to be ~3000 GM (based upon the measured one photon 30% quantum yield for activated clusters[47]). This is a large TPA cross-section value, which promotes the possibility of using the DNA–Ag NCs for multi-photon imaging. The steady state emission at 540 nm is not observed for Ag NC on ssDNA or dsDNA under two-photon excitation. Two-photon excited fluorescence at 630 nm was observed only for Ag NC on dsDNA, detailed in Fig. 6. The steady state absorption spectrum (Fig. 1) shows that at the same concentration, absorption at 400 nm is stronger for Ag NC on ssDNA, yet Ag NC on ssDNA did not possess detectable two-photon excited fluorescence at 650 nm. There are two possible explanations. (1) It is possible that two-photon absorption is stronger for Ag NC on ssDNA, but the transition state for the 650 nm emission is not present, which suggests that the proximity to a tunable enhancer gives rise to such a state. (2) Ag on ssDNA is not two-photon active and the proximity of the enhancer sequence will cause a geometric or electronic change that gives rise to two-photon allowed transition. However, the excitation spectrum indicates that the emission at 650 nm is strongly related to the transition at 580 nm, suggesting that the lack of an emissive state for Ag on ssDNA is the more likely case.

### E. Wavelength resolved femtosecond transient absorption

Transient absorption was used to investigate the excited state dynamics of DNA–Ag NCs. Transient absorption measures the difference between excited state absorption and steady state absorption using pump probe spectroscopy. The change in absorption is measured in the ultrafast time scale of 200 fs to 1600 ps, producing excited state dynamics information at the probe wavelength of 450 nm to 750 nm. Attempts to measure DNA–Ag NC transient absorption under 350 nm excitation suffered from sample degradation. Excited with a 470 nm pump beam, the transient absorption spectrum (Fig. 7) displayed

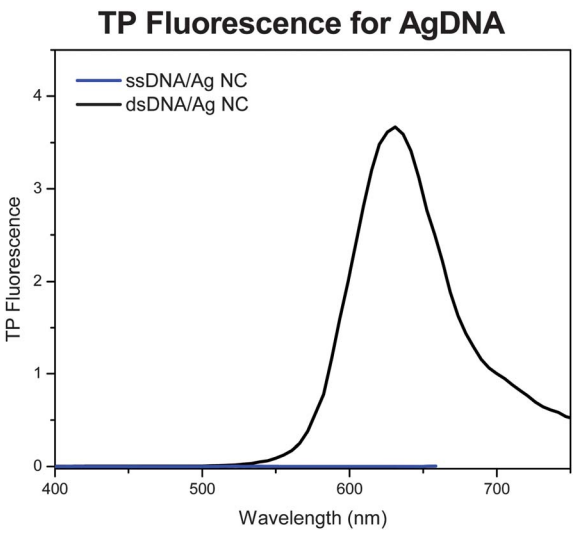


**Fig. 5** Two photon fluorescence emission spectra for DNA–Ag NC systems under 800 nm excitation.

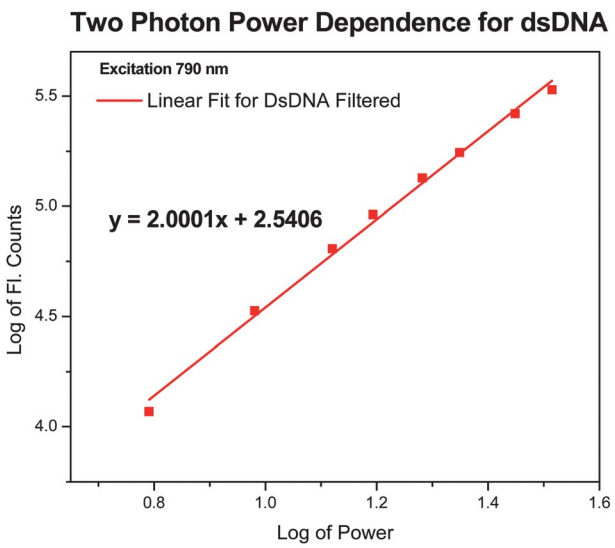


**Fig. 6** Two photon power dependence for DNA–Ag NC systems.

a strong excited state absorption (ESA) at ~560 nm for both Ag NCs on ssDNA and dsDNA (Fig. 8).

We investigated the transient absorption kinetics of Ag NC on both ssDNA and dsDNA (Fig. 8 and 9). Kinetics fitting was performed with the Surface Xplorer software supplied by Ultrafast systems. The dynamics of the systems at 565 nm are similar for both Ag NC on ssDNA and dsDNA. The feature at 565 nm has a very short rise time that cannot be resolved by the instrument (~150 fs). It also has a long decay time of a few hundred ps. The long decay time indicates discrete energy levels typical of nanoclusters. The board transient absorption feature suggests a combination of excited states at similar wavelengths. When the enhancer sequence is introduced to form Ag NC on dsDNA, an excited state feature is observed at 590 nm (Fig. 7). The kinetics (Fig. 9) shows a non-positive value before zero time (excitation) for the peak at 590 nm, indicating that it is a bleached state that has a longer lifetime than the laser repetition rate (1 kHz) of 1 ms or longer. After the zero time, the bleach structure shows a similar rise time compared to the peak at 565 nm (Fig. 9). However, the ESA peak at 565 nm is very broad (Fig. 7), covering the bleach state's wavelength at 590 nm. The decay to zero for the 565 nm bleach after excitation is the result of the rising ESA signal, masking the bleach signal; therefore kinetics observed for the bleach is independent of the ESA, suggesting that the two excited states are entirely different. Previous investigations done by Moran *et al.*[28] on Au NCs have shown that bleach states in transient absorption can be matched to absorption peaks of the steady absorption spectrum. It is interesting to see that the bleach signal at 590 nm for Ag NC on dsDNA can be matched to the absorption peak at 590 nm (Fig. 10), suggesting that the two states are related. The peak at 590 nm also overlaps with the 580 nm peak for the excitation spectrum, so the emission at 650 nm is directly related to the bleached excited state at 590 nm. Therefore, the enhancer sequence creates a new excited state at 590 nm and is directly related to the emission at 650 nm. This is a first report of an emission related excited state for MPCs detected by transience absorption. The enhancer sequence is crucial to the emitting nanoclusters in the Ag NC on dsDNA.

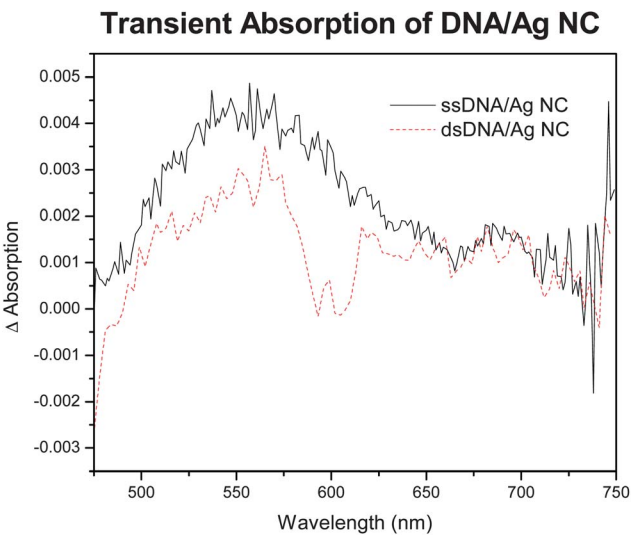


**Fig. 7** Transient absorption of ssDNA and dsDNA at ~20 ps.

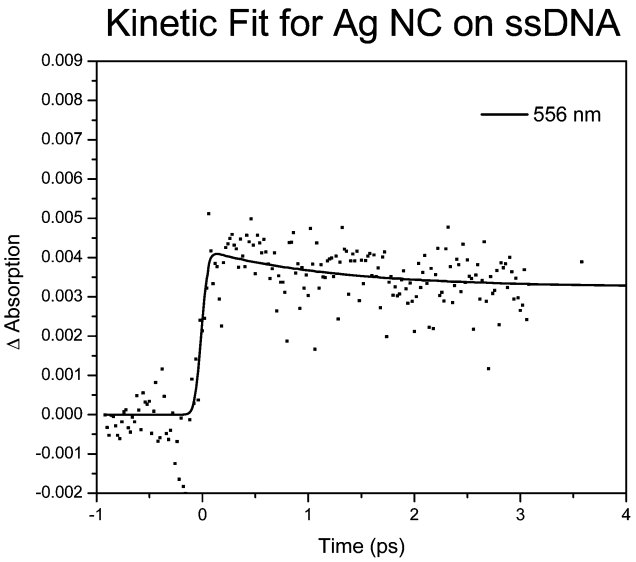


**Fig. 8** Kinetic fit for Ag NC on ssDNA at 556 nm.

### F. Mechanism of emissions

The steady state emission spectrum recorded two different emissions at 540 nm and 650 nm (Fig. 2). Time-resolved fluorescence experiments indicate that the emission at 650 nm is a single-exponential decay with a lifetime of 4 ns compared to the bi-exponential decay at 540 nm.[36] In our previous investigations,[56] similar dynamics were observed for larger Ag and Au particles, and the bi-exponential decay was assigned to the fluorescence originating from the recombination of electrons in the s–p band with holes in the d band. However, the long fluorescence lifetime observed for the DNA–Ag NC systems suggests that the dynamics are associated with nanoclusters. The largest amplitude of emission for DNA–Ag NC systems is at 650 nm. Given the strength and long lifetime of the emission, we propose that this emission originates from the surface states of the

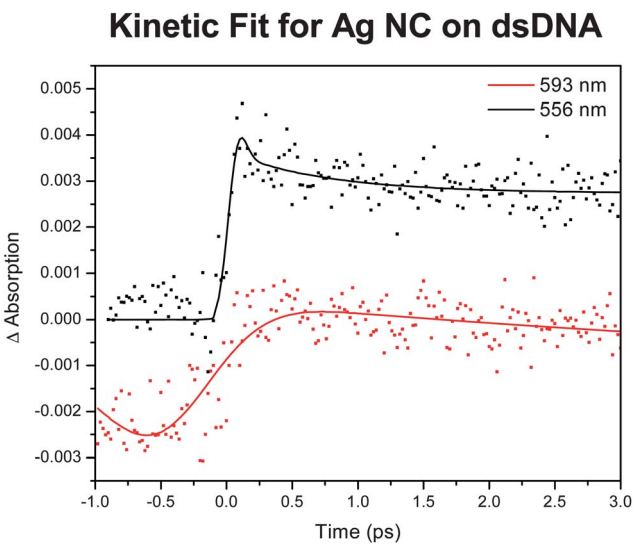


**Fig. 9** Transient absorption kinetic fit for Ag NC on dsDNA at 692 nm and 556 nm.

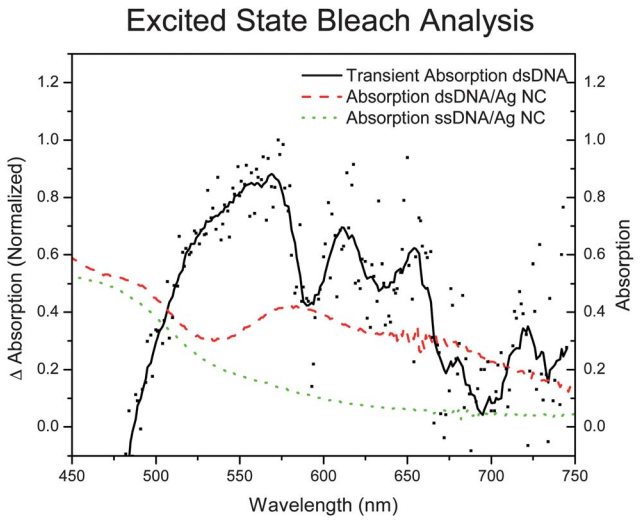


**Fig. 10** Excited bleach observed at 590 nm corresponds (see text for detail identification of the bleach) to the absorption peak at 590 nm for Ag NC on dsDNA.

nanoclusters, similar to NIR emission for Au NCs.[8,20] From the excitation spectrum, the observed emission at 650 nm is related to the transition at 590 nm. From our analysis, the transition at 590 nm is related to the absorption peak at 580 nm. Hence the emission at 650 nm is due to the excited state at 590 nm, and the presence of nanoclusters in the system.

The surface state emission for the nanoclusters is attributed to the interaction between the metal core and the outer ligand (thiolate) shell.[19,21,28] Previous reports have shown that the core and the shell do not interact chemically,[21,57] but an increase in the polarization of the ligand shell affects the emission of MPCs.[53] We also suggest that the outer organic layer acts as a field to introduce polarization to the metal core. It is important to treat the metal core as a single "super atom", and therefore can be treated as a system with discrete energy levels. The relatively long lifetime of the energy levels leads to the emission from MPCs. More details on modeling of the effect of polarization are needed to further understand this effect. While DNA–Ag NCs do not have a thiolate shell that surrounds the metal cluster, the DNA binds the cluster and could provide a similar polarizing environment to the Ag NC. It was shown that the emission from DNA–Ag NCs is enhanced by the introduction of a guanine-rich tail ($3'$-$G_4(TG_4)_2TG_3$) on the complementary DNA strand.[36] From previous reports, the emission enhancement for Nano-Cluster Beacons is the strongest at the guanine-rich tail, while emission from a cytosine-rich tail is much weaker.[36] A comparison of guanine and cytosine reveals that the larger size of guanine could potentially polarize the metal core as a "super atom", even if cytosine has a stronger dipole. The greater enhancement from guanine is consistent with the idea that an induced polarization to the nanoclusters strongly affects their emission properties.

According to the steady state absorption, emission, time-resolved emission and transient absorption data, we propose two different emission mechanisms for Ag NCs on dsDNA detailed in Fig. 11. The emission at 540 nm may be caused by NPs and NCs in the system, but lifetime analysis suggests that the system

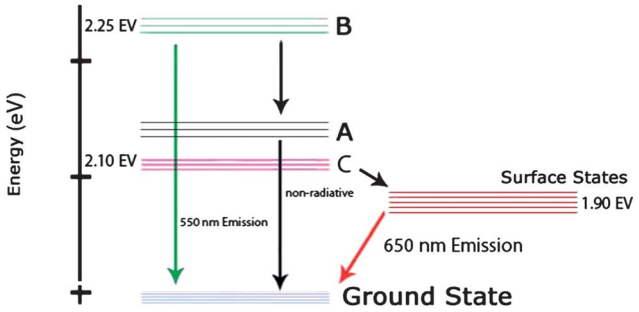


**Fig. 11** Proposed energy structure for dsDNA Ag nanoclusters.

is more similar to nanoclusters than nanoparticles. The emission mechanism can be explained by a simple four level system (Fig. 11). Based on our model, the emission at 540 nm originates from the B state (associated with the metal core) and the emission at 650 nm comes from the surface state. The introduction of the enhancer sequence to the Ag NC creates a new electronic state C, observed in transient absorption as an excited state bleach. State C directly relates to the absorption at 590 nm and attributes to the large emission at 650 nm. The large emission observed is due to the highly efficient energy transfer between the 590 nm absorption and the surface state emission. It is possible that the excited state C is itself the emissive state (or state C is the surface state), with the current experiment information available we separate the states to illustrate that state C can be a possible core state, hence different from the surface state. However, we are certain that the large enhanced emission is caused by the new excited state (state C) created by the enhancer sequence upon hybridization.

## IV. Summary

In summary, DNA–Ag NC systems offer many interesting optical properties. Ag NCs on ssDNA have an absorption peak that is similar to the SPR response for nanoparticles (2.2 nm), with the formation of the dsDNA system resulting in a decrease in the absorption. Discrete absorption features are observed for dsDNA which demonstrates the presence of a quantum size effect. Emission was measured for DNA–Ag NCs using steady state and time resolved techniques. Two different emission features were recorded: a core emission at 550 nm was shared by both Ag NC on ssDNA and dsDNA; a stronger surface state emission at 650 nm is only observed for Ag NC on dsDNA. An enhancement in emission by the hybridization of the ssDNA by a complementary strand with a guanine-rich tail is observed. Time-resolved fluorescence is observed at 550 nm with a lifetime of 1 ps and 17 ps; the decay lifetime is longer than for nanoparticles. We suggest that the polarization of nanoclusters by the enhancer sequence is critical to emission observed at 650 nm. The enhancer sequence also creates a new excited state observed at 590 nm in the transient absorption spectrum. Additionally, the excited state at 590 nm is directly related to the emission. Based on the emission and steady state results, we model the emission mechanism of Ag NCs on dsDNA with a four-level system. Two-photon excited fluorescence with emission at 630 nm was also observed for the first time for DNA-templated metal clusters, and the large cross-section calculated encourages the use of

DNA–Ag NCs as a bio-imaging tool. We are also excited to report the observation of an excited state in the transient absorption spectrum after 1.5 ps at 590 nm that is directly related to the emission enhancement of nanoclusters, resulting from the possible polarization of the super-atom by an enhancer with a guanine-rich tail.

## Acknowledgements

We acknowledge support by the Army Research Office (T. G. III, Materials) Department of Energy, Office of Basic Energy Sciences, Division of Materials Sciences and Engineering and PECASE (A.P.S., J.S., and J.S.M.) and the Los Alamos National Laboratory Research LDRD-DR program (J.H.W and H.-C.Y.). This work was partially performed at the Center for Integrated Nanotechnologies, a U.S. Department of Energy, Office of Basic Energy Sciences user facility at Los Alamos National Laboratory (contract DE-AC52-06NA25396).

## References

1 R. Murray, *Chem. Rev.*, 2008, **108**, 2688.
2 G. Schmid, *Chem. Soc. Rev.*, 2008, **37**, 1909.
3 J. Zheng, C. Zhang and M. Dickson, *Phys. Rev. Lett.*, 2004, **93**, 077402.
4 M. Walter, J. Akola, O. Lopez-Aceedo, P. D. Jadzinsky, G. Calero, C. J. Ackerson, R. L. Whetten, H. Gronbeck and H. Hakkinen, *Proc. Natl. Acad. Sci. U. S. A.*, 2008, **105**, 9157.
5 O. P. Varnavski, T. Goodson III, M. B. Mohamed and M. A. El-Sayed, *Phys. Rev. A: At., Mol., Opt. Phys.*, 2005, **72**, 235405.
6 G. Ramakrishna, Q. Dai, J. Zou, Q. Huo and T. Goodson, *J. Am. Chem. Soc.*, 2007, **129**, 1848.
7 G. Ramakrishna, O. Varnavski, J. Kim, D. Lee and T. Goodson, *J. Am. Chem. Soc.*, 2008, **130**, 5032.
8 S. H. Yau, O. Varnavski, J. D. Gilbertson, B. Chandler, G. Ramakrishna and T. GoodsonIII, *J. Phys. Chem. C*, 2010, **114**, 15979.
9 S. Antonello, A. H. Holm, E. Instuli and F. Maran, *J. Am. Chem. Soc.*, 2007, **129**, 9836.
10 L. Pasquato, P. Pengo and P. Scrimin, *J. Mater. Chem.*, 2004, **14**, 3481.
11 N. Zheng and G. D. Stucky, *J. Am. Chem. Soc.*, 2006, **128**, 14278.
12 M. Valden, X. Lai and D. W. Goodman, *Science*, 1998, **281**, 1647.
13 M. Tuner, V. B. Golovoko, O. P. H. Vaughan, P. Abdulkin, A. Berenguer-Murcia, M. S. Tikhov, B. F. G. Johnson and R. M. Lamber, *Nature*, 2008, **454**, 981.
14 C. Long, J. D. Gilbertson, G. Vijayaraghavan, K. J. Stevenson, C. J. Pursell and B. D. Chandler, *J. Am. Chem. Soc.*, 2008, **130**, 10103.
15 H. Lang, R. A. May, B. L. Iversen and B. D. Chandler, *J. Am. Chem. Soc.*, 2003, **125**, 14832.
16 J. F. Hainfield, *Science*, 1987, **236**, 450.
17 J. M. Nam, C. S. Thaxton and C. A. Mirkin, *Science*, 2003, **301**, 1884.
18 S. Chen, R. S. Ingram, M. J. Hostetler, J. J. Pietron, R. W. Murray, T. G. Schaaff, J. T. Khoury, M. M. Alvarez and R. L. Whetten, *Science*, 1998, **280**, 2098.
19 M. Zhu, C. M. Aikens, F. J. Hollander, G. C. Schatz and R. Jin, *J. Am. Chem. Soc.*, 2008, **130**, 5883.
20 Y. Negishi, N. K. Chaki, Y. Shichibe, R. L. Whetten and T. Tsukuda, *J. Am. Chem. Soc.*, 2007, **129**, 11322.
21 T. Kim, S. Oh and R. Crooks, *Chem. Mater.*, 2004, **16**, 167.
22 J. D. Gilbertson, G. Vijayaraghavan, K. J. Steverson and B. D. Chandler, *Langmuir*, 2007, **23**, 11239.
23 P. D. Jadzinsky, G. Calero, C. J. Ackerson, D. A. Bushnell and R. R. Kornberg, *Science*, 2007, **314**, 430.
24 R. L. Whetten and R. C. Price, *Science*, 2007, **318**, 407.
25 M. W. Heaven, A. Dass, P. S. White, K. M. Holt and R. W. Murray, *J. Am. Chem. Soc.*, 2008, **130**, 3754.
26 J. Akola, M. Walter, R. L. Whetten, H. Hakkinen and H. Gronbeck, *J. Am. Chem. Soc.*, 2008, **130**, 3756.
27 T. G. Schaaff, G. Knight, M. N. Shafigullin, R. F. Borkman and R. L. Whetten, *J. Phys. Chem. B*, 1998, **102**, 10643.
28 S. A. Miller, J. M. Womick, J. F. Parker, R. W. Murray and A. M. Moran, *J. Phys. Chem. C*, 2009, **113**, 9440.
29 B. A. Smith, J. Z. Zhang, U. Giebel and G. Schmid, *Chem. Phys. Lett.*, 1997, **270**, 139.
30 R. G. Ispasoiu, L. Balogh, O. P. Varnavski, D. A. Tomalia and T. Goodson, *J. Am. Chem. Soc.*, 2000, **122**, 11005.
31 T. Goodson III, O. Varnavski and Y. Wang, *Int. Rev. Phys. Chem.*, 2004, **23**, 109, Soc.
32 R. B. Wyrwas, M. M. Alvarez, J. T. Khoury, R. C. Price, T. G. Schaaff and R. L. Whetten, *Eur. Phys. J. D*, 2007, **43**, 91.
33 S. Kumar, M. D. Bolan and T. P. Bigioni, *J. Am. Chem. Soc.*, 2010, **38**, 13141.
34 I. G. Dance, K. J. Fisher, R. M. Herath Banda and M. L. Scudder, *Inorg. Chem.*, 1991, **30**, 183.
35 J. Sharma, H. C. Yeh, H. Yoo, J. H. Werner and J. Martinez, *Chem. Commun.*, 2010, **46**, 3280.
36 H. C. Yeh, J. Sharma, J. Han, J. Martinez and J. Werner, *Nano Lett.*, 2010, **10**, 3106.
37 M. Neidig, J. Sharma, H. C. Yeh, J. Martinez, S. Conradson and A. Shreve, *J. Am. Chem. Soc.*, 2011, **133**, 11837.
38 J. Sharma, H. C. Yeh, H. Yoo, J. Werner and J. Martinez, *Chem. Commun.*, 2011, **47**, 2294.
39 J. Y. Petty, J. Zheng, N. V. Hud and R. M. Dickson, *J. Am. Chem. Soc.*, 2004, **126**, 5207.
40 C. I. Richards, S. Choi, J.-C. Hsiang, Y. Antoku, T. Vosch, A. Bongiorno, Y.-L. Tzeng and R. M. Dickson, *J. Am. Chem. Soc.*, 2008, **130**, 5038.
41 E. G. Gwinn, P. O'Neil, A. J. Guerrero, D. Bouwmeester and D. k. Fygenson, *Adv. Mater.*, 2008, **20**, 279.
42 T. Vosch, Y. Antoku, J.-C. Hsiang, C. I. Richards, J. I. Gonzales and R. M. Dickson, *Proc. Natl. Acad. Sci. U. S. A.*, 2007, **104**, 12616.
43 J. Sharma, H.-C. Yeh, H. Yoo, J. H. Werner and J. S. Martinez, *Chem. Commun.*, 2010, **46**, 3280.
44 J. T. Petty, C. Fan, S. P. Story, B. Sengupta, A. S. J. Iyer, Z. Prudowsky and R. M. Dickson, *J. Phys. Chem. Lett.*, 2010, **1**, 2524.
45 P. R. O'Neill, L. R. Velazquez, D. G. Dunn, E. G. Gwinn and D. K. Fygenson, *J. Phys. Chem. C.*, 2009, **113**, 4229.
46 J. T. Petty, C. Fan, S. P. Story, B. Sengupta, A. S. J. Iyer, Z. Prudowsky and R. M. Dickson, *J. Phys. Chem. Lett.*, 2010, **1**(17), 2524.
47 H. C. Yeh, personal communication, manuscript in preparation.
48 C. M. Aikens, *J. Phys. Chem. C*, 2008, **112**, 19797.
49 C. M. Aikens, *J. Phys. Chem. A*, 2009, **113**, 10811.
50 A. Bhasker, G. Ramakrishna, Z. Lu, R. Twieg, J. M. Hales, D. J. Haga, E. Van Stryland and T. Goodson, III, *J. Am. Chem. Soc.*, 2006, **128**, 11840.
51 G. Ramakrishna, A. Bhaskar and T. Goodson, III, *J. Phys. Chem. B*, 2006, **110**, 20872.
52 C. Xu and W. W. Webb, *J. Opt. Soc. Am. B*, 1996, **13**, 481.
53 S. Peng, J. M. McMahon, G. Schatz, S. K. Gray and Y. Sun, *Proc. Natl. Acad. Sci. U. S. A.*, 2010, **107**, 14530.
54 C. M. Aikens, *J. Phys. Chem. Lett.*, 2011, **2**, 104.
55 A. Mooradian, *Phys. Rev. Lett.*, 1969, **22**, 185.
56 O. Varnavski, R. G. Ispasoiu, L. Balogh, D. Tomalia and T. Goodson III, *J. Chem. Phys.*, 2001, **114**, 1962.
57 G. Wang, T. Huang, R. W. Murray, L. Menard and R. G. Nuzzo, *J. Am. Chem. Soc.*, 2005, **127**, 812.
58 M. B. Mohamed, V. Volkov, S. Link and M. A. El-Sayed, *Chem. Phys. Lett.*, 2000, **317**, 517.
59 T. Huang and R. W. Murray, *J. Phys. Chem. B*, 2003, **107**, 7434.
60 T. P. Bigioni, R. L. Whetten and O. Dag, *J. Phys. Chem. B*, 2000, **104**, 6983.
61 G. Wang, R. Guo, G. Kalyuzhny, J. Choi and R. Murray, *J. Phys. Chem. B*, 2006, **110**, 20282.

 